Electronic Supplementary Material (ESI) for New Journal of Chemistry.

Supplementary Information

A new heterogeneous host-guest catalytic system as an eco-friendly approach for the synthesis of cyclic carbonates from CO_2 and epoxides

Anaïs Mirabaud,[a,b] Alexandre Martinez,[c] François Bayard,[a] Jean-Pierre Dutasta,*[b] Véronique Dufaud*[a]

[a] *Laboratoire de Chimie, Catalyse, Polymères, Procédés (C2P2), CNRS, Université Claude Bernard Lyon 1, CPE Lyon, 43 Bd du 11 novembre 1918, F-69616 Villeurbanne cedex, France*

[b] *Laboratoire de Chimie, École Normale Supérieure de Lyon, CNRS, Université Claude Bernard Lyon 1, 46 allée d'Italie, F-69364 Lyon, France*

[c] *Aix Marseille Université, Centrale Marseille, CNRS, iSm2 UMR 7313, F-13397 Marseille, France*

Corresponding Authors: E-mail: veronique.dufaud@univ-lyon1.fr; jean-pierre.dutasta@ens-lyon.fr

Content Page

Characterization of azidopropyl and cavitand based hybrid materials

Table S1. Physical and textural properties of azidopropyl and triphosphonate cavitand containing hybrid silica materials

Materials	d_{100}[a] [Å]	a_0[b] [Å]	Wall thickness[c] [Å]	V_p[d] [$cm^3.g^{-1}$]	D_p[e] [Å]	S_{BET} [$m^2.g^{-1}$]	C_{BET}
UL-SBA-15	126	145	48	1.5	97	597	222
[N_3]/UL-SBA-15	125	144	49	1.3	95	508	107
[3*i*PO]/UL-SBA-15	125	144	61	0.9	83	378	55

[a] d(100) spacing. [b] $a_0 = 2d(100)/\sqrt{3}$ hexagonal lattice parameter calculated from XRD. [c] Calculated by a_0 – pore size. [d] Total pore volume at P/P0 = 0.973. [e] Pore size from desorption branch applying the BJH pore analysis.

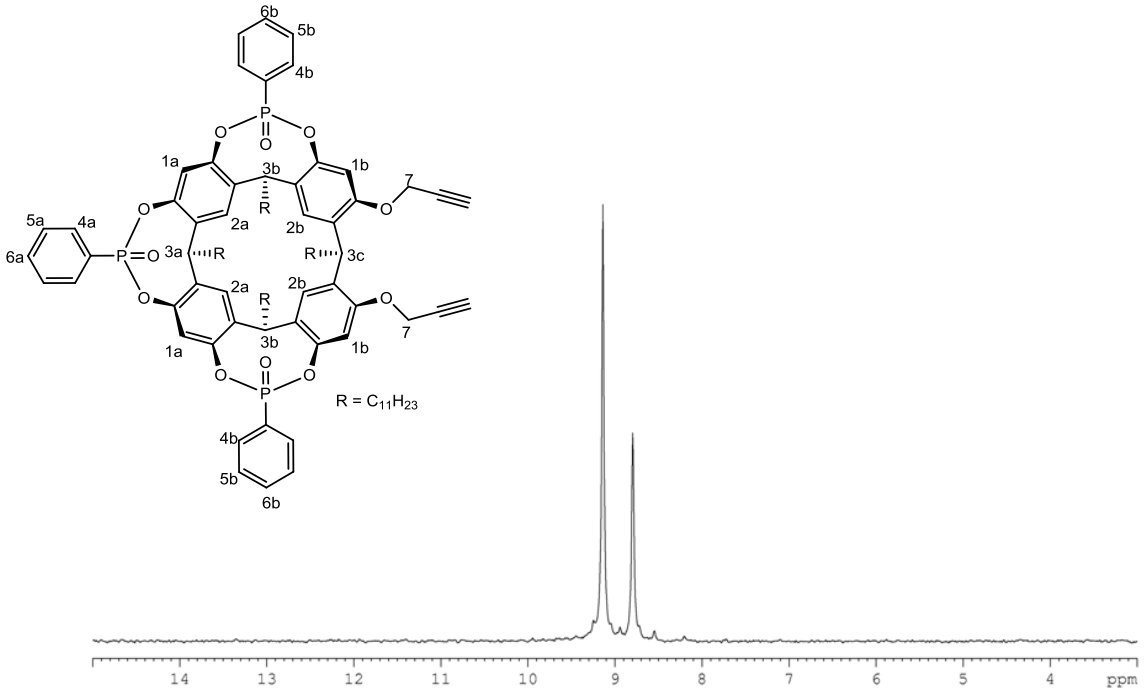

Figure S1. Liquid ^{31}P NMR spectrum ($CDCl_3$, 298 K, 202.4 MHz) of triphosphonate cavitand **[3*i*PO]**.

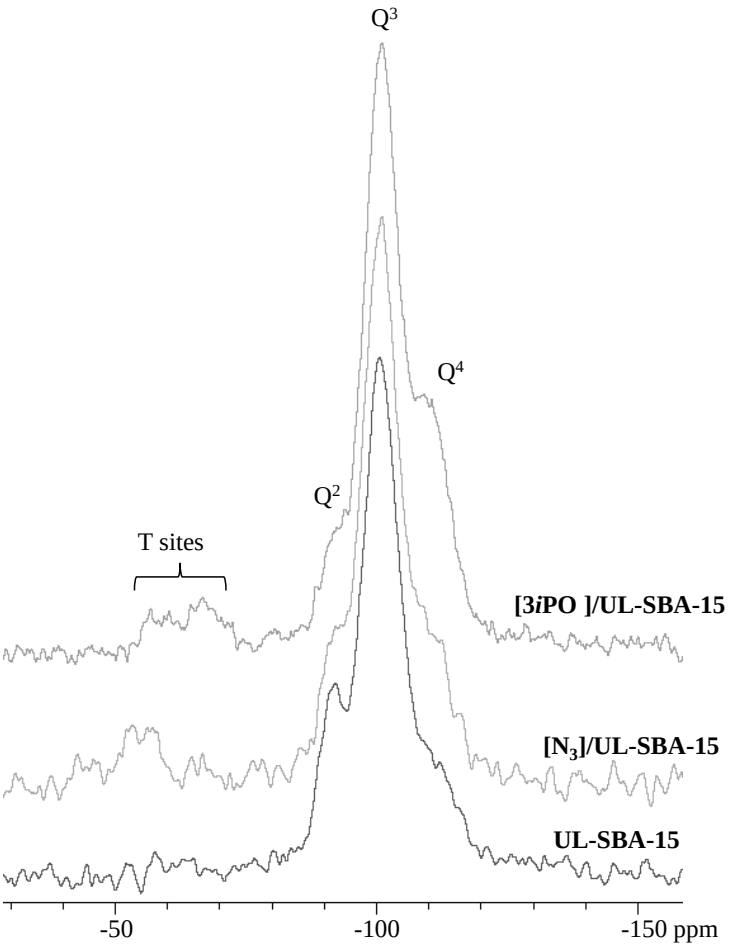

Figure S2. CP MAS ^{29}Si NMR of **[N_3]/UL-SBA-15** before and after clicking cavitand **[3*i*PO]** and of native **UL-SBA-15** silica.

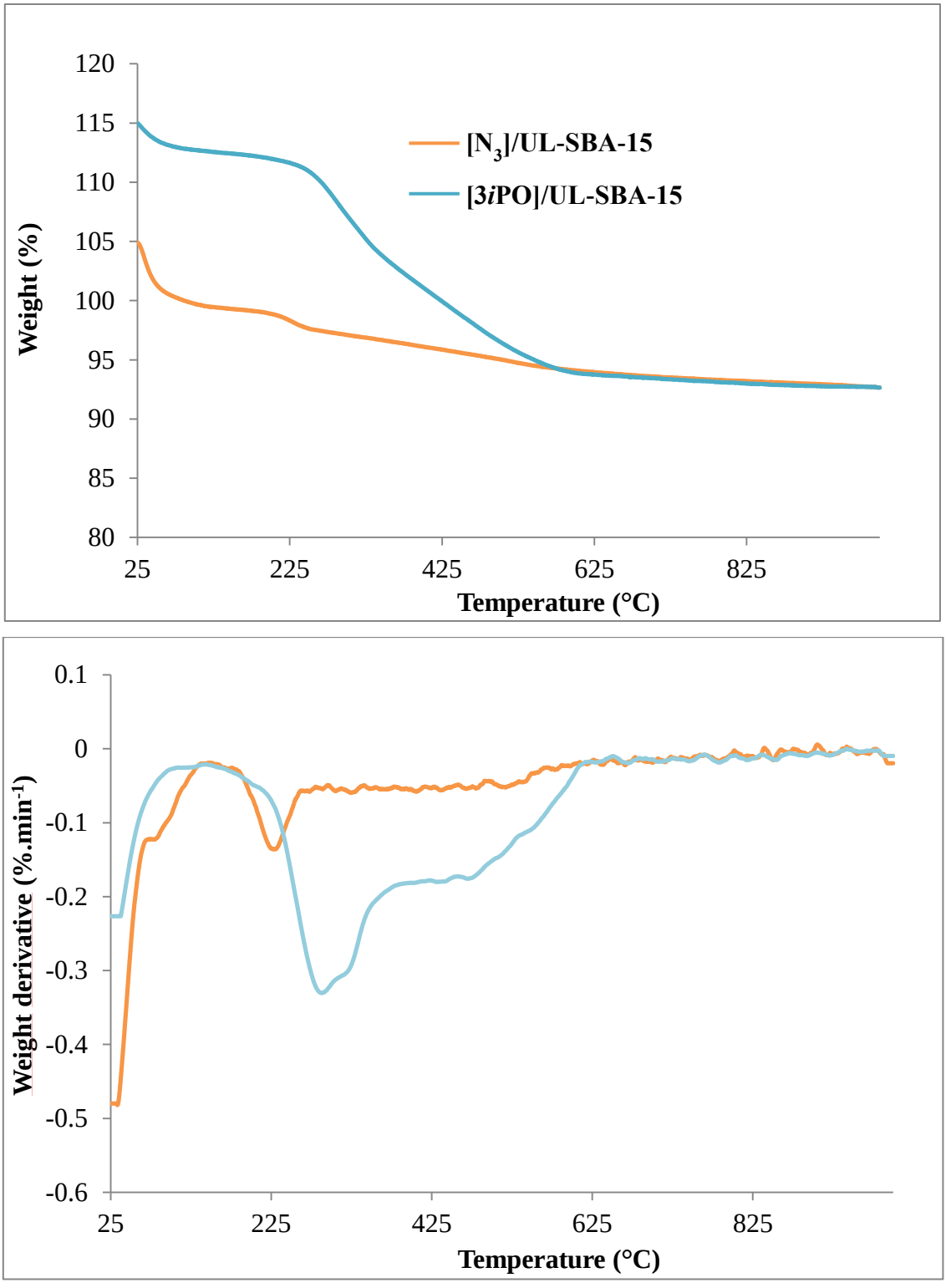

Figure S3. Representative thermogravimetric weight loss curves and derivatives plots for **[N_3]/UL-SBA-15** and **[3*i*PO]/UL-SBA-15**. The TGA weight loss curves were normalized using dry silica weight as the reference (i.e. the weight at the end of the TGA run, 900°C) to correct for differences in water content.

Table S2. Comparison of the quantitative data derived from elemental analysis and TGA measurements

	TGA[a]	Microanalysis only	Microanalysis corrected using TGA[a]
	mmol·g^{-1} dry silica	mmol·g^{-1} hybrid	mmol·g^{-1} dry silica
[N_3]/UL-SBA-15	0.38	0.29[b]	0.32
[3*i*PO]/UL-SBA-15	0.10	0.086[c]	0.11

[a] SiO_2 content in the solid was derived from the value of dry mineral analyzed by TGA/DTA at 900 °C. [b] Derived from N analysis (N: 1.2 %$_{wt}$). [c] Derived from P analysis (P: 0.8 %$_{wt}$).

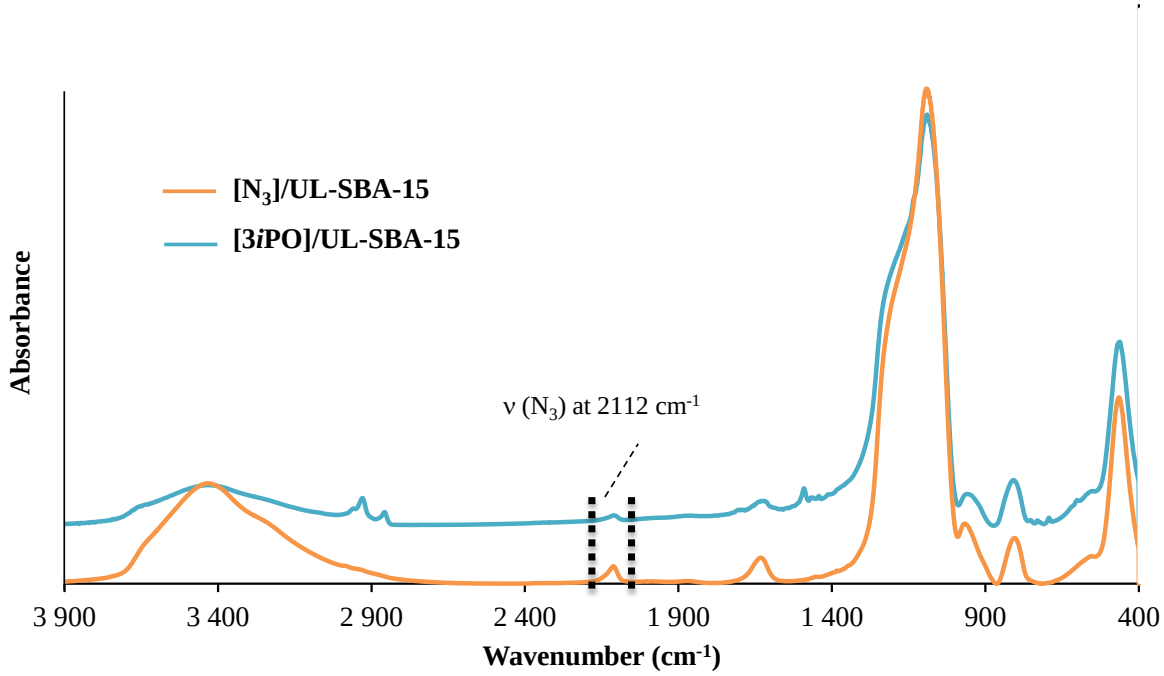

Figure S4. FT-IR spectra of **[N_3]/UL-SBA-15** and **[3*i*PO]/UL-SBA-15**.

Characterization of ammonium based hybrid material

Table S3. Physical and textural properties of native silica and of propyltrimethylammonium chloride containing hybrid silica materials

Materials	N [%wt]	Cl [%wt]	d_{100}[a] [Å]	a_0[b] [Å]	Wall thickness[c] [Å]	V_p[d] [$cm^3.g^{-1}$]	D_p[e] [Å]	S_{BET} [$m^2.g^{-1}$]	C_{BET}
SBA-15	-		101	117	51	1.2	66	916	164
[N^+]/SBA-15 LL	0.28	0.58	100	116	51	1.0	65	746	108
[N^+]/SBA-15 HL	1.34	2.73	97	112	59	0.7	53	492	81
UL-SBA-15	-		126	145	48	1.5	97	618	222
[N^+]/UL-SBA-15 LL	0.3	0.56	127	147	51	1.4	96	492	131
[N^+]/UL-SBA-15 HL	0.63	1.79	126	145	54	1.2	91	437	105
SiO_2	-		-	-	-	-	-	201	95
[N^+]/SiO_2 LL	0.33	0.73	-	-	-	-	-	199	82
[N^+]/SiO_2 HL	0.51	1.07	-	-	-	-	-	166	76

[a] d(100) spacing. [b] $a_0 = 2d(100)/\sqrt{3}$ hexagonal lattice parameter calculated from XRD. [c] Calculated by a_0 – pore size. [d] Total pore volume at P/P0 = 0.973. [e] Pore size from desorption branch applying the BJH pore analysis.

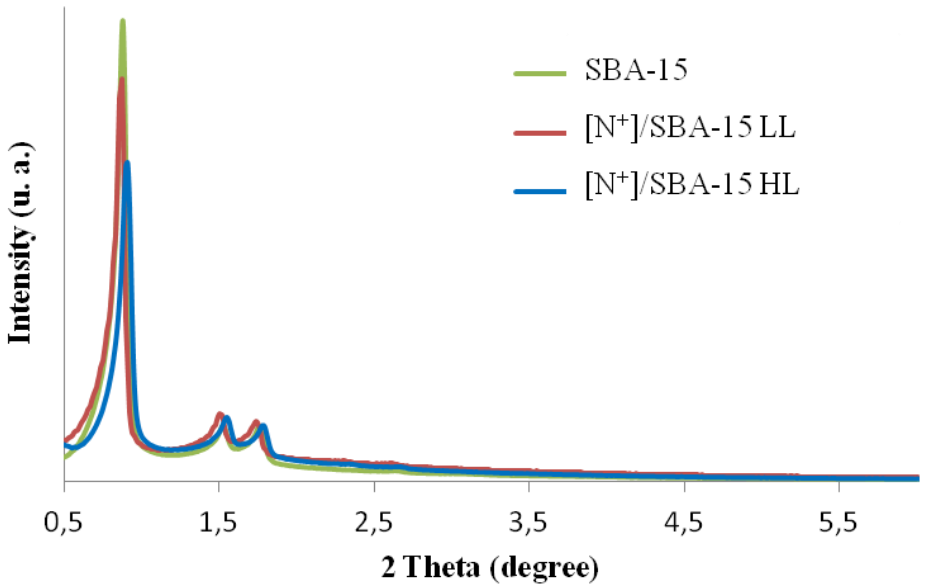

Figure S5. X-ray powder diffraction patterns of ammonium functionalized SBA-15 silica materials and of parent SBA-15.

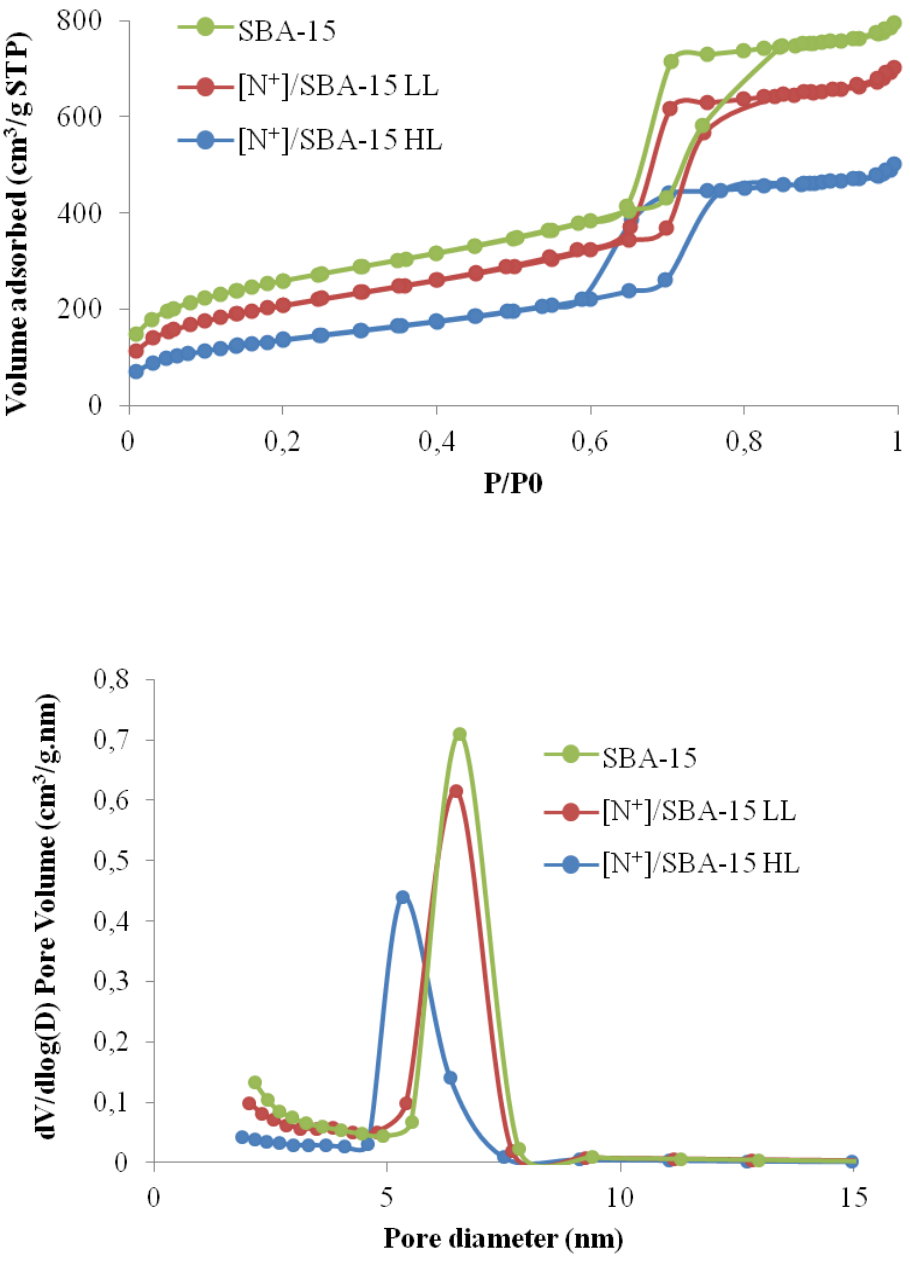

Figure S6. Nitrogen adsorption-desorption isotherms (top) and pore size distributions (bottom) of ammonium functionalized SBA-15 silica materials and of parent SBA-15.

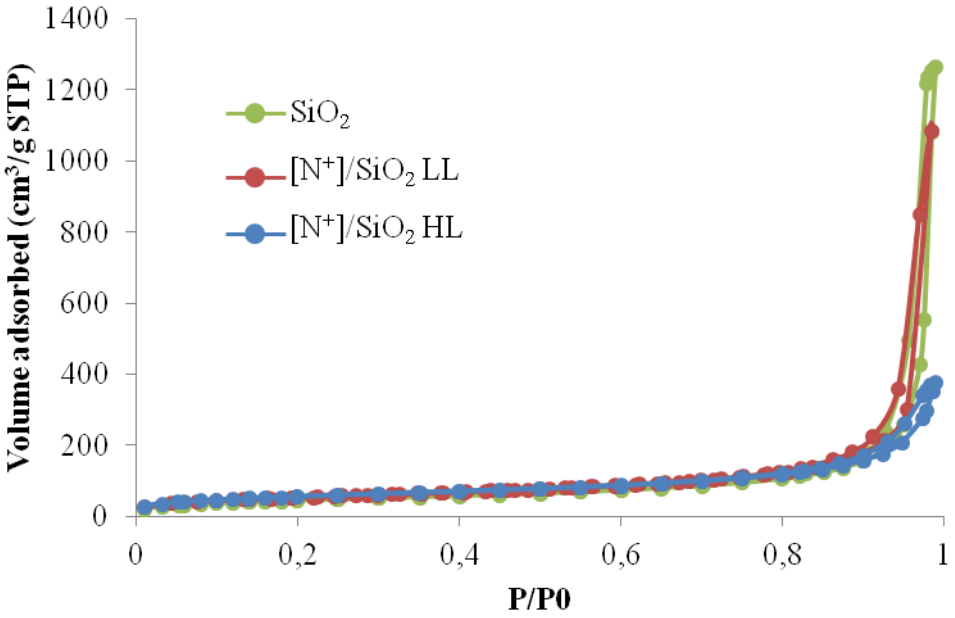

Figure S7. Nitrogen adsorption-desorption isotherms of ammonium functionalized non-porous SiO_2 materials and of parent SiO_2.

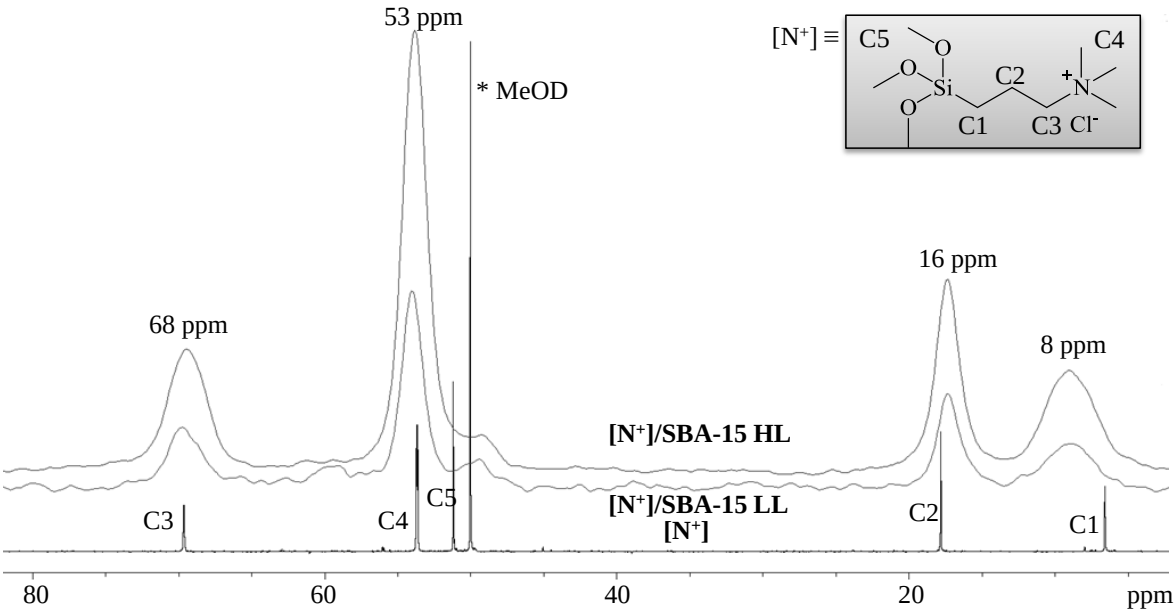

Figure S8. CP MAS ^{13}C NMR of ammonium hybrid materials based on SBA-15 and liquid ^{13}C NMR of molecular N-[3-(trimethoxysilyl)propyl]-N.N.N-trimethylammonium chloride precursor.

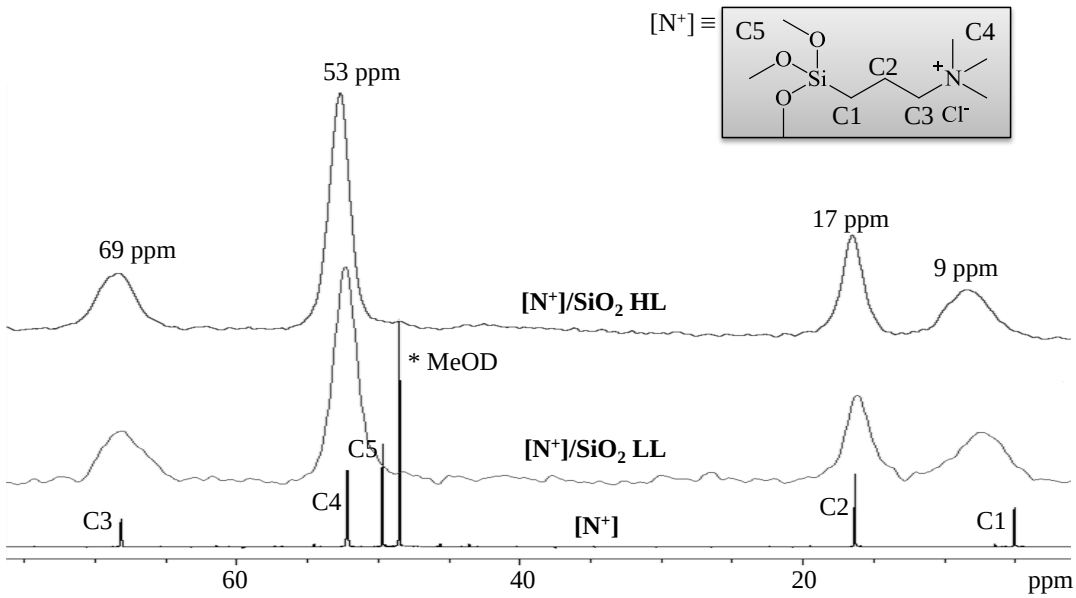

Figure S9. CP MAS ^{13}C NMR of ammonium hybrid materials based on non-porous SiO_2 and liquid ^{13}C NMR of molecular N-[3-(trimethoxysilyl)propyl]-N.N.N-trimethylammonium chloride precursor.

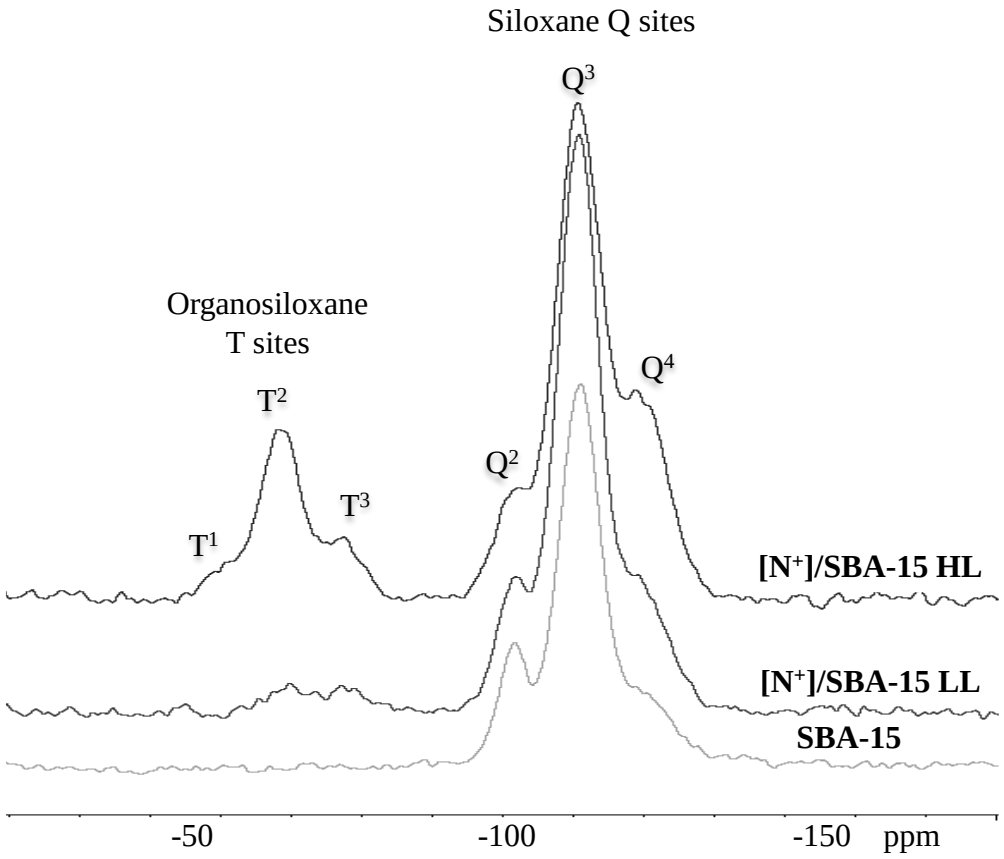

Figure S10. CP MAS ^{29}Si NMR of ammonium hybrid materials based on SBA-15 silica and of native SBA-15.

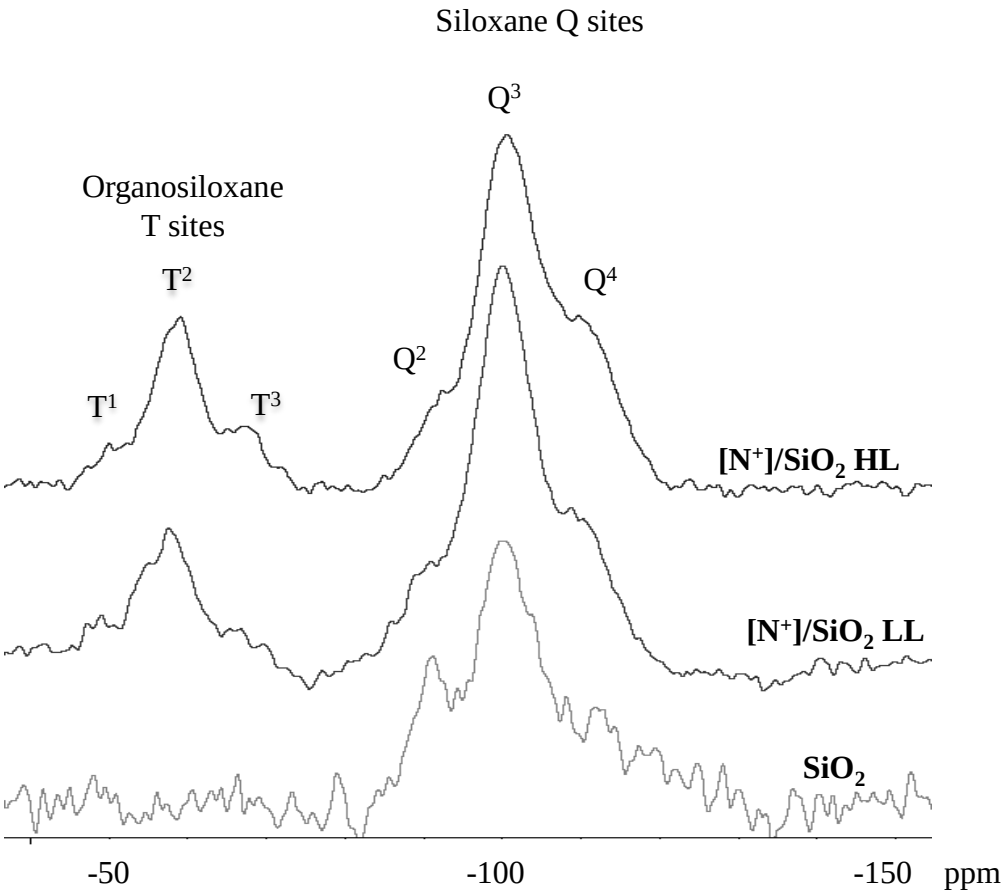

Figure S11. CP MAS ^{29}Si NMR of ammonium hybrid materials based on non-porous SiO_2 and of native SiO_2.

Table S4. Nitrogen and chlorine elemental analyses for ammonium based hybrid materials.

Materials	**N [wt. %]**	**%Cl [wt. %]**
[N$^+$]/SBA-15 LL	0.28 ± 0.03	0.58 ± 0.06
[N$^+$]/SBA-15 HL	1.34 ± 0.13	2.73 ± 0.27
[N$^+$]/UL-SBA-15 LL	0.30 ± 0.03	0.56 ± 0.06
[N$^+$]/UL-SBA-15 HL	0.63 ± 0.06	1.79 ± 0.18
[N$^+$]/SiO$_2$ LL	0.33 ± 0.03	0.73 ± 0.07
[N$^+$]/SiO$_2$ HL	0.51 ± 0.05	1.07 ± 0.11

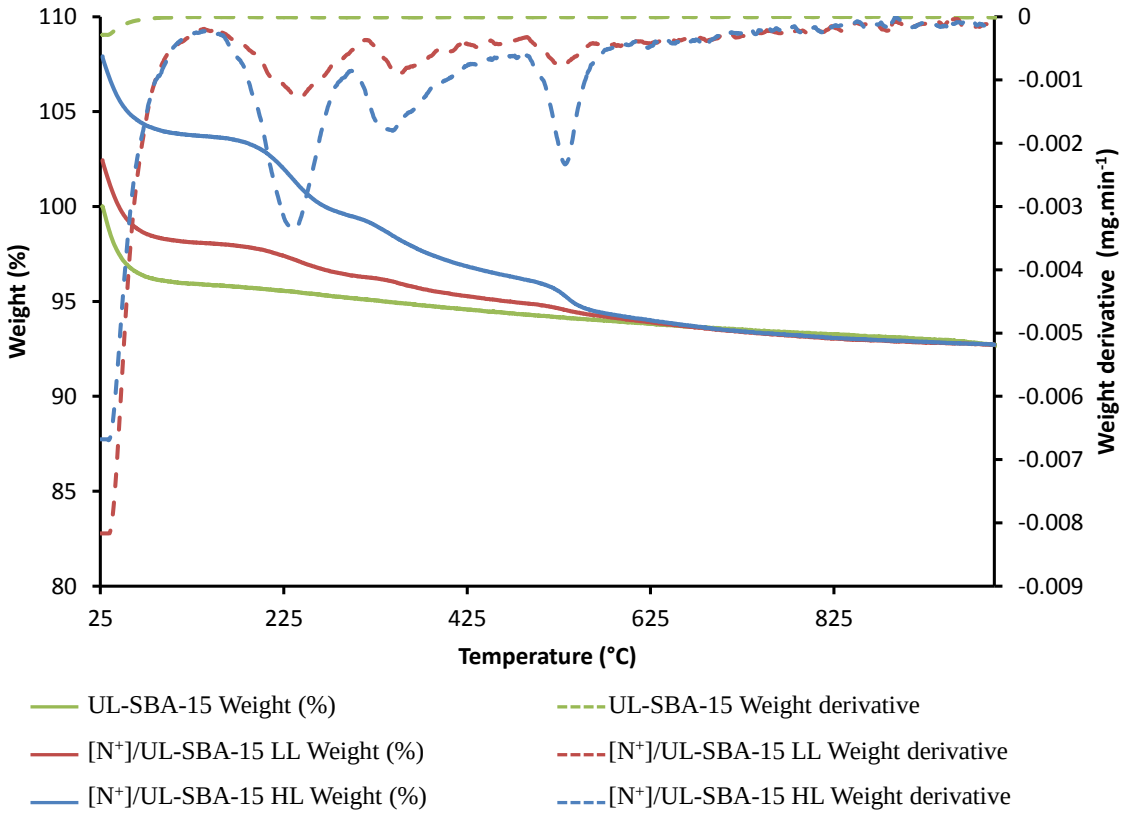

Figure S12. Representative thermogravimetric weight loss curves and derivatives plots for ammonium hybrid materials based on UL-SBA-15 silica. The TGA weight loss curves were normalized using dry silica weight as the reference (i.e. the weight at the end of the TGA run, 900°C) to correct for sample humidity.

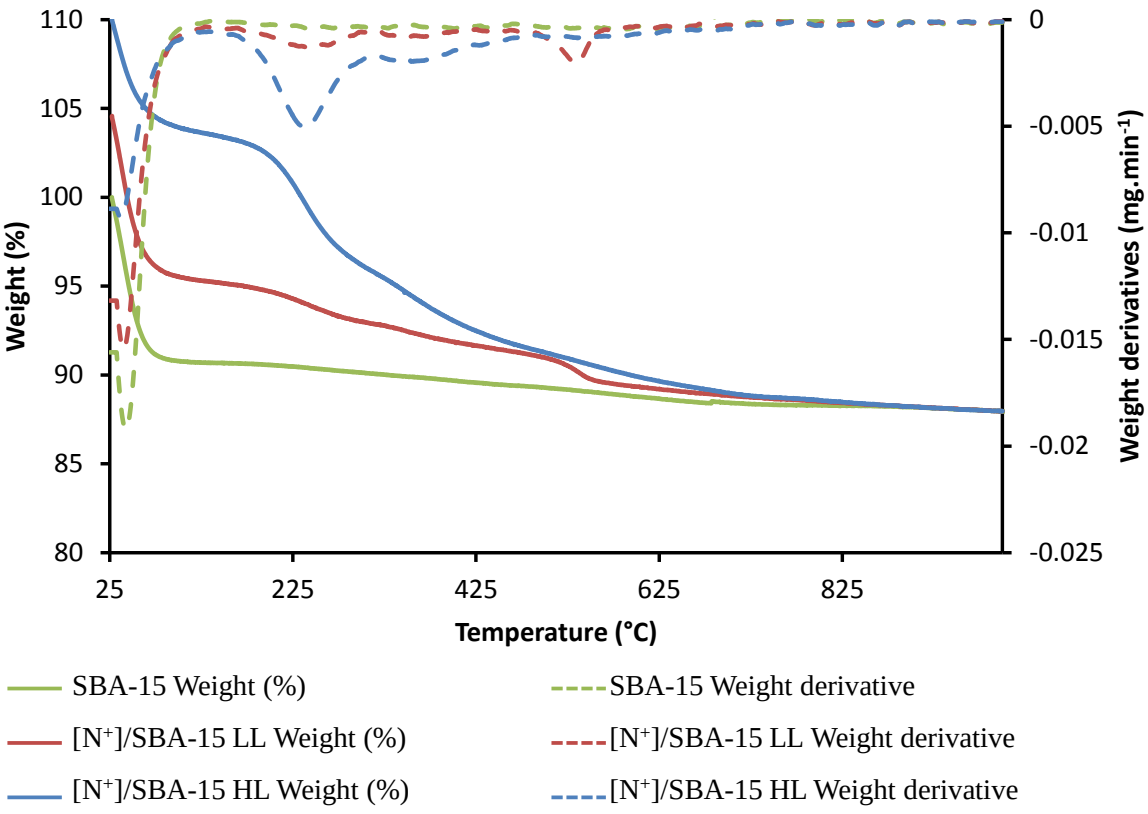

Figure S13. Representative thermogravimetric weight loss curves and derivatives plots for ammonium hybrid materials based on SBA-15 silica. The TGA weight loss curves were normalized using dry silica weight as the reference (i.e. the weight at the end of the TGA run, 900°C) to correct for sample humidity.

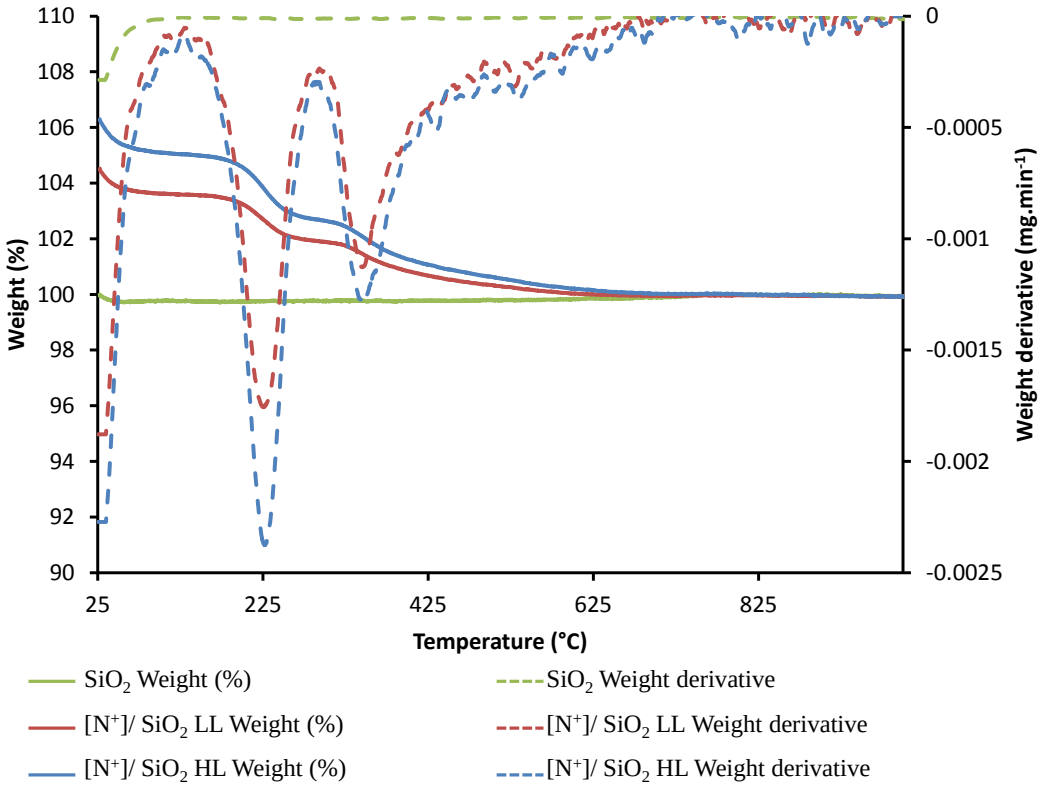

Figure S14. Representative thermogravimetric weight loss curves and derivatives plots for ammonium hybrid materials based on non-porous SiO_2. The TGA weight loss curves were normalized using dry silica weight as the reference (i.e. the weight at the end of the TGA run, 900°C) to correct for sample humidity.

Table S5. TGA weight loss for ammonium based hybrid materials.

Materials	**Residual mass at 900 °C [%]**	**Weight loss[a] [%]**		
		25-130 °C	**130-600 °C**	**600-900 °C**
[N⁺]/SBA-15 LL	84.11	10.33	6.75	1.57
[N⁺]/SBA-15 HL	79.93	7.12	15.54	2.23
[N⁺]/UL-SBA-15 LL	90.51	4.51	4.38	1.42
[N⁺]/UL-SBA-15 HL	85.92	4.33	10.32	1.57
[N⁺]/SiO_2 LL	95.60	0.87	3.57	0.11
[N⁺]/SiO_2 HL	94.01	1.20	4.85	0.28

[a] Relative to dry silica weight at 900 °C.

Catalytic testing

Table S6. Experimental details for the coupling of CO_2 with styrene oxide catalysed by tetrabutylammonium iodide in the presence of cavitand functionalized material and native silica.

Co-catalyst	Loading [mmol [3*i*PO].g^{-1}]	Mass introduced [mg]
native UL-SBA-15	-	333
[N_3]/UL-SBA-15	-	333
[3*i*PO]/UL-SBA-15	0.11	333

Table S7. Experimental details for the coupling of CO_2 with styrene oxide catalyzed by propyltrimethylammonium chloride functionalized silica materials.

Catalyst	Loading [mmol [N^+].g^{-1}]	Mass introduced [mg]
[N^+]/SBA-15 LL	0.24	167
[N^+]/UL-SBA-15 LL	0.24	167
[N^+]/SiO_2 LL	0.25	167
[N^+]/SBA-15 HL	1.20	33
[N^+]/UL-SBA-15 HL	0.52	77
[N^+]/SiO_2 HL	0.39	103

Table S8. Experimental details for the coupling of CO_2 with styrene oxide catalyzed by propyltrimethylammonium chloride functionalized silica materials in the presence of cavitand **[4*i*PO]** co-catalyst.

Catalyst	Loading [mmol [N^+].g^{-1}]	Mass introduced [mg]
[N^+]/UL-SBA-15 HL	0.52	77
[N^+]/SiO_2 LL	0.25	167
[N^+]/SiO_2 HL	0.39	103
[N^+]/UL-SBA-15 LL	0.24	167